APPLIED MECHANICS 2018
April 9 - 11, 2018, Myslovice, Czech republic

RECENT PROGRESS IN NUMERICAL METHODS FOR EXPLICIT FINITE ELEMENT ANALYSIS

R. Kolman[1], J. Kopačka [2], J. Gonzalez[3], D. Gabriel[4], S.S. Cho[5], J. Plešek[6], K.C. Park[7]

Abstract: In this paper, a recent progress in explicit finite element analysis is discussed. Properties and behaviour of classical explicit time integration in finite element analysis of elastic wave propagation and contact-impact problems based on penalty method in contact-impact problems are summarized. Further, stability properties of explicit time scheme and the penalty method as well as existence of spurious oscillations in transient dynamics are mentioned. The novel and recent improving and progress in explicit analysis based on a local time integration with pullback interpolation for different local stable time step sizes, bipenalty stabilization for enforcing of contact constrains with preserving of stability limit for contact-free problems and using a direct inversion of mass matrix are presented. Properties of the employed methods are shown for one-dimensional cases of wave propagation and contact-impact problems.

Keywords: Explicit time integration; Finite element method, Penalty and Bipenalty method; Direct inversion of mass matrix; Local time stepping; Spurious oscillations.

1 Introduction

Although explicit finite element analysis has a long tradition and it is widely implemented in commercial FEM software and used in real applications, it is still necessary to improve this technology and develop new methods and procedures. In many cases, implementations of explicit finite element method are based on linear finite element type with reduced one-point integration and hourglass stabilization, with lumped (diagonal) mass matrix and the central difference method in time [1, 2]. There are some shortcomings in addressing wave propagation in solids and modelling of contact-impact problems, where the penalty method is often used [3]. The list of disadvantages of explicit finite element analysis with traditional methods could be mentioned as motivation for improving:

- existence of spurious oscillations of stresses for computations with small time step sizes,
- loss of accuracy in computations of waves propagation in heterogeneous materials with different wave speeds,
- influence of stability limit by the stiffness penalty term for enforcing of contact constrains and requirement for optimal setting of the stiffness penalty parameter [3].

[1] Radek Kolman; Institute of Thermomechanics, The Czech Academy of Sciences, Dolejškova 5, Prague, 182 00, Czech Republic; kolman@it.cas.cz

[2] Ján Kopačka; Institute of Thermomechanics, The Czech Academy of Sciences, Dolejškova 5 Prague, 182 00, Czech Republic; kopacka@it.cas.cz

[3] Jose Gonzalez; Escuela Técnica Superior de Ingeniería, Universidad de Sevilla, Camino de los Descubrimientos s/n Seville, E-41092, Spain; japerez@us.es

[4] Dušan Gabriel; Institute of Thermomechanics, The Czech Academy of Sciences, Dolejškova 5 Prague, 182 00, Czech Republic; gabriel@it.cas.cz

[5] Sang Soon Cho; Reactor Mechanical Engineering, Division, Korea Atomic Energy Research Institute, Daejeon, 305-353, 999-111, Daedeok-Daero, Yuseong-gu, Republic of Korea; e-mail: sscho96@kaist.ac.kr

[6] Jiří Plešek; Institute of Thermomechanics, The Czech Academy of Sciences, Dolejškova 5, Prague, 182 00, Czech Republic; plesek@it.cas.cz

[7] K.C. Park; Department of Aerospace Engineering, Sciences, University of Colorado at Boulder, Boulder, 80309-429, CO, USA; kcpark@colorado.edu

2 Explicit time integration in FEM

In this paper, the main attention is paid to explicit time integration in finite element method, for details see [2, 4]. We shortly introduce the basic idea of this method for solving of a dynamic system. After finite element discretization [5], the equation of motion has the form

$$\mathbf{M}\mathbf{a} = \mathbf{f}_{ext} - \mathbf{f}_{int} - \mathbf{f}_{cont} \tag{1}$$

where $\mathbf{M}$ is the mass matrix, $\mathbf{a}$ is the vector of nodal accelerations, $\mathbf{f}_{ext}$, $\mathbf{f}_{int}$ and $\mathbf{f}_{cont}$ are the vectors of external, internal and contact forces, respectively. In the following text, $\mathbf{u}$, $\mathbf{v} = \dot{\mathbf{u}}$ and $\mathbf{a} = \ddot{\mathbf{u}}$ mark the vectors of nodal displacements, velocities and accelerations. In linear theory, the internal forces are computed as $\mathbf{f}_{int} = \mathbf{K}\mathbf{u}$, where $\mathbf{K}$ is the stiffness matrix. We assume the finite element method with linear shape functions and lumped mass matrix given by row-summing of terms.

In this paper, we present a predictor-corrector form of the central difference method in time. The predictor-corrector form of the central difference method [2] to solve a general dynamic problem (1) with geometrical and material non-linearities is briefly listed below.
Predictor phase:

$$\begin{aligned} \tilde{\mathbf{u}}^{n+1} &= \mathbf{u}^n + \Delta t \dot{\mathbf{u}}^n + \frac{\Delta t^2}{2}\ddot{\mathbf{u}}^n \\ \dot{\tilde{\mathbf{u}}}^{n+1} &= \dot{\mathbf{u}}^n + \frac{\Delta t}{2}\ddot{\mathbf{u}}^n \\ \ddot{\tilde{\mathbf{u}}}^{n+1} &= \mathbf{0} \end{aligned} \tag{2}$$

The system of equations of motion constituted at the time $t^{n+1} = t^n + \Delta t$ to solve:

$$\mathbf{M}^{n+1}(\tilde{\mathbf{u}}^{n+1}, t^{n+1})\Delta\ddot{\tilde{\mathbf{u}}}^{n+1} = \mathbf{f}_{ext}(t^{n+1}) - \mathbf{f}_{int}(\tilde{\mathbf{u}}^{n+1}, \dot{\tilde{\mathbf{u}}}^{n+1}, t^{n+1}) - \mathbf{f}_{cont}(\tilde{\mathbf{u}}^{n+1}, \dot{\tilde{\mathbf{u}}}^{n+1}, t^{n+1}) \tag{3}$$

Corrector phase:

$$\begin{aligned} \mathbf{u}^{n+1} &= \tilde{\mathbf{u}}^{n+1} \\ \dot{\mathbf{u}}^{n+1} &= \dot{\tilde{\mathbf{u}}}^{n+1} + \frac{\Delta t}{2}\Delta\ddot{\tilde{\mathbf{u}}}^{n+1} \\ \ddot{\mathbf{u}}^{n+1} &= \Delta\ddot{\tilde{\mathbf{u}}}^{n+1} \end{aligned} \tag{4}$$

Here $\Delta\ddot{\tilde{\mathbf{u}}}^{n+1}$ marks the update acceleration vector and Δt is the time step size. Quantities with the superscript n has a meaning of the approximation of quantities at the time t^n, e.g. $\mathbf{u}^n \approx \mathbf{u}(t^n)$ and so on. In the foregoing relationships, the predictor quantities are marked by the tilde.

Generally, explicit methods are only conditionally stable; the time step size Δt has to satisfy a stability limit in the form $\Delta t \leq \Delta t_c$, where Δt_c is the critical time step size. The critical time step size securing the stability of the central difference method for a linear undamped system takes the form [6]

$$\Delta t_c = \frac{2}{\omega_{max}} \tag{5}$$

where ω_{max} being the maximum eigenfrequency of the system, related to the generalized eigen-value problem $\mathbf{K}\mathbf{u} = \lambda\mathbf{M}\mathbf{u}$, taking $\omega^2 = \lambda$, see [1, 6].

In real multi-dimensional cases, the critical time step size Δt_c could be exactly determined with respect to Eq (5), but it is practically impossible to compute ω_{max} for a large eigen-value problem of linearized system at each time step. On the other hand, we know, by Fried's theorem [7], that the maximum frequency ω_{max} is bounded by ω^e_{max} obtained as the maximum eigen-value taken over all the elements in a FE mesh. In wave propagation problem in solids, the stable time step size satisfying the stability limit is approximately equal to the time required to run longitudinal elastic wave through the

smallest finite element constituting a FE mesh [2]. For some element types and uniform FE meshes, the critical time step size is estimated under elastic wave propagation rule of thumb $\Delta t_c = \alpha H/c_L$ [1], where H is the characteristic length of the smallest element of a FE mesh and α is a parameter depending on finite element type and its shape.

An example of stress wave propagation in an elastic bar for different time step sizes defines by the Courant number $Co = \Delta t c_L/H$ is shown in Fig. 1. Here, one can see spurious oscillations in stress distributions in a bar, which are a by-product of dispersive behaviour of the finite element method. For the critical Courant number $Co = 1$, the results for the linear finite element with the lumped mass matrix show disperionless behaviour.

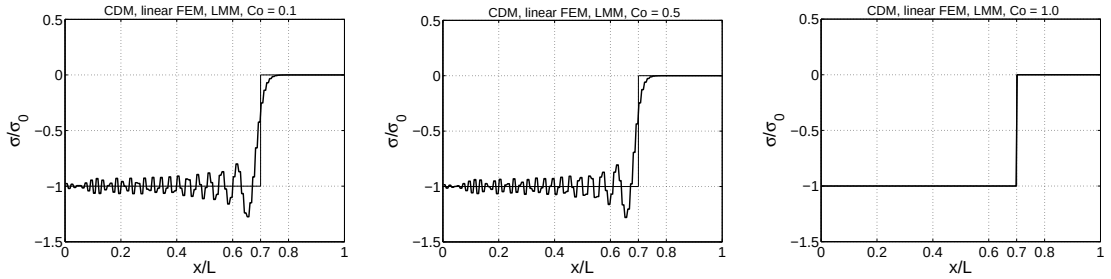

Figure 1: Example of stress wave propagation in an elastic bar for different time step sizes.

3 Recent numerical methods in explicit time integration

In the following text, the recent modifications and novel methods in explicit time integration applied on problems of wave propagation and contact-impact problems of solids are mentioned and presented as follows:

- Explicit time integration with local time stepping [8]
- Bipenalty method in contact-impact problems [9]
- Direct inversion of mass matrix [10]

3.1 Explicit time integration with local time stepping

In this section, we present a special time stepping process for wave propagation in heterogeneous media, where different wave speeds at different positions of a body are assumed. The presented numerical method for wave propagation in heterogeneous materials is based on the algorithm presented by Park in [11, 12]. This scheme has been reformulated into the two-time step scheme in [13]. The used time stepping process is consisted of following two computational steps for the predictor-corrector form for numerically elimination of spurious stress oscillations close to wavefront and dispersive properties of the finite element method [14] as follows:

STEP 1. Pull-back integration with local stepping:

1a) Integration by the central difference scheme with the local (elemental) critical time step size Δt_e^{cr} for each finite element at the time $t^{n+cr} = t^n + \Delta t_e^{cr}$

$$(\mathbf{u}_{fs}^{n+cr})_e = \mathbf{u}_e^n + \Delta t_e^{cr}\mathbf{v}_e^n + \frac{1}{2}(\Delta t_e^{cr})^2\mathbf{a}_e^n \tag{6}$$

$$(\mathbf{a}_{fs}^{n+cr})_e = (\mathbf{M}_e)^{-1}\left[\mathbf{f}_e^{n+cr} - \mathbf{K}_e(\mathbf{u}_{fs}^{n+cr})_e\right] \tag{7}$$

The elemental critical time step size Δt_e^{cr} is set as $\Delta t_e^{cr} = h_e/c_e$ or $\Delta t_e^{cr} = 2/\omega_{max}^e$, where ω_{max}^e is the maximum eigen-angular velocity for the e-th separate finite element. Here $\mathbf{K}_e$ and $\mathbf{M}_e$ are elemental stiffness and mass matrices.

1b) Pull-back interpolation of local nodal displacement vectors at the time $t^{n+1} = t^n + \Delta t$ with $\alpha = \Delta t/\Delta t_e^{cr}$, $\quad \beta_1(\alpha) = \frac{1}{6}\alpha\big(1 + 3\alpha - \alpha^2\big)$, $\quad \beta_2(\alpha) = \frac{1}{6}\alpha\big(\alpha^2 - 1\big)$

$$(\mathbf{u}_{fs}^{n+1})_e = \mathbf{u}_e^n + \Delta t_e^{cr}\mathbf{v}_e^n + (\Delta t_e^{cr})^2\beta_1\mathbf{a}_e^n + (\Delta t_e^{cr})^2\beta_2(\mathbf{a}_{fs}^{n+cr})_e \tag{8}$$

1c) Assembling of local contributions of displacement vector from Step 1b.

$$\mathbf{u}_{fs}^{n+1} = [\mathbf{L}^{\mathrm{T}}\mathbf{L}]^{-1}\mathbf{L}^{\mathrm{T}}(\mathbf{u}_{fs}^{n+1})_e \tag{9}$$

where $\mathbf{L}$ is the assembly Boolean matrix.

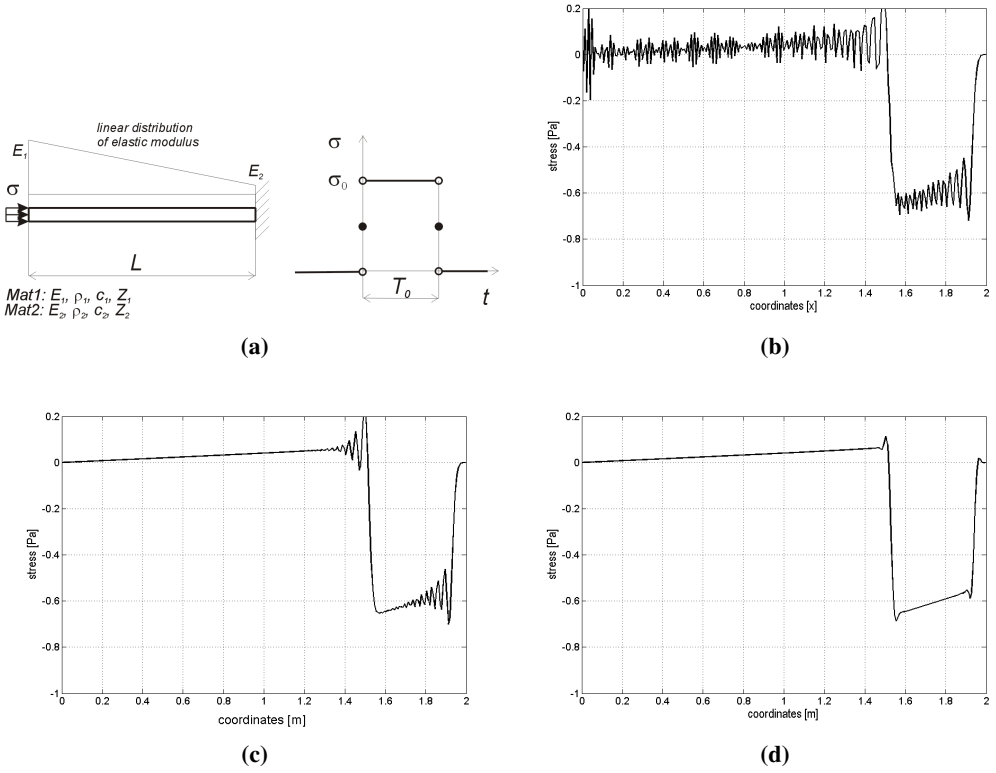

Figure 2: a) Scheme of a free-fixed graded elastic bar under shock loading. Stress distributions in a graded elastic bar under shock loading obtained by b) the central difference method, c) the Park method without local stepping, d) the Park method with local stepping. Corresponding Courant number $Co = 0.5$ and $\theta = 0.5$.

STEP 2. Push-forward integration with averaging:

2a) Push-forward predictor of displacement vector at the time $t^{n+1} = t^n + \Delta t$ by the central difference scheme with the time step size Δt.

$$\mathbf{u}_{cd}^{n+1} = \mathbf{u}^n + \Delta t\mathbf{v}^n + \frac{1}{2}\Delta t^2\mathbf{a}^n \tag{10}$$

2b) Averaging of the total displacement vectors at the time $t^{n+1} = t^n + \Delta t$ from Steps 1c and 2a for given $\theta = [0, 1]$.

$$\mathbf{u}^{n+1} = \theta \mathbf{u}_{fs}^{n+1} + (1-\theta)\mathbf{u}_{cd}^{n+1} \tag{11}$$

2c) Evaluation of acceleration and velocity nodal vectors at the time $t^{n+1} = t^n + \Delta t$.

$$\mathbf{a}^{n+1} = (\mathbf{M})^{-1}\left[\mathbf{f}(t^{n+1}) - \mathbf{K}\mathbf{u}^{n+1}\right] \tag{12}$$

$$\mathbf{v}^{n+1} = \mathbf{v}^n + \frac{1}{2}(\mathbf{a}^n + \mathbf{a}^{n+1}) \tag{13}$$

An example of results of numerical solution of elastic wave propagation problem in a graded bar is presented in Fig. 2a. The elastic modulus of a bar is linearly distributed along the bar, where $E_1 = 16$ Pa and $E_2 = 1$ Pa. The density is constant along the bar. The presented explicit scheme with local time stepping produces results without spurious oscillations, but only small cusps on the corners of stress discontinuities can be observed, see Figs. 2. Further, the improvement of stress spurious oscillations is evident with comparison of the scheme with and without local stepping, because the nominated local stepping process respects local critical time step at each material point.

3.2 Bipenalty method in finite element method for contact-impact problems

In the work [9], the improving of the penalty method based on the bipenalty modification in application into dynamic contact problems has been presented with the stability analysis. In the bipenalty method, beside the additional penalized stiffness term as in the penalty method corresponding to penetration of bodies, an additional penalized mass term is added and contact residual forces are computed as

$$\hat{\mathbf{R}}_{\mathrm{c}}(\hat{\mathbf{u}}, \ddot{\hat{\mathbf{u}}}) = \hat{\mathbf{M}}_{\mathrm{p}}\ddot{\hat{\mathbf{u}}} + \hat{\mathbf{K}}_{\mathrm{p}}\hat{\mathbf{u}} + \hat{\mathbf{f}}_{\mathrm{p}} \tag{14}$$

where

$$\hat{\mathbf{M}}_{\mathrm{p}} = \int_{\Gamma_{\mathrm{c}}} \epsilon_{\mathrm{m}} H(g)\mathbf{N}\mathbf{N}^{\mathrm{T}}\,\mathrm{d}S \qquad \hat{\mathbf{K}}_{\mathrm{p}} = \int_{\Gamma_{\mathrm{c}}} \epsilon_{\mathrm{s}} H(g)\mathbf{N}\mathbf{N}^{\mathrm{T}}\,\mathrm{d}S \qquad \hat{\mathbf{f}}_{\mathrm{p}} = \int_{\Gamma_{\mathrm{c}}} \epsilon_{\mathrm{s}} H(g)\mathbf{N}g_0\,\mathrm{d}S \tag{15}$$

Here, $\hat{\mathbf{M}}_{\mathrm{p}}$ is the additional elemental mass matrix due to inertia penalty, $\hat{\mathbf{K}}_{\mathrm{p}}$ is the additional elemental stiffness matrix due to stiffness penalty, $\hat{\mathbf{u}}$ is the vector of displacements of contact pairs and $\hat{\mathbf{f}}_{\mathrm{p}}$ is the part of the elemental contact force due to the initial gap g_0; g is the gap function; $H(g)$ is the Heaviside step function for prescribing active or inactive contact constraints; ϵ_{m} and ϵ_{s} are mass and stiffness penalty parameters; Γ_{c} is the contact surface between bodies; the matrix $\mathbf{N}$ represents an operator from the displacement field $\mathbf{u}$ to the gap function g_{N} in the contact

$$g_{\mathrm{N}} = \mathbf{N}^{\mathrm{T}}\mathbf{u} + g_0. \tag{16}$$

The particular form of the matrix $\mathbf{N}$ follows from the used contact discretization.

We now consider the time integration of the semi-discretized system (1) in the framework of the central difference method

$$(\mathbf{M}^t + \mathbf{M}_{\mathrm{p}}^t)\frac{\mathbf{u}^{t+\Delta t} - 2\mathbf{u}^t + \mathbf{u}^{t-\Delta t}}{\Delta t^2} + (\mathbf{K}^t + \mathbf{K}_{\mathrm{p}}^t)\mathbf{u}^t + \mathbf{f}_{\mathrm{p}}^t - \mathbf{R}^t = \mathbf{0} \tag{17}$$

Assuming that displacements are known at time $t - \Delta t$ and t, one can resolve unknown displacements at time $t + \Delta t$, where Δt marks the time step size. Note, that the matrices $\mathbf{M}_{\mathrm{p}}^t$ and $\mathbf{K}_{\mathrm{p}}^t$ are time-dependent because they are associated with active contact constraints.

The stability graph for several combination of mass and stiffness penalty parameters is presented in Fig. 3, for more details see [9]. One can see the stability limit for the penalty limit and the stability limit

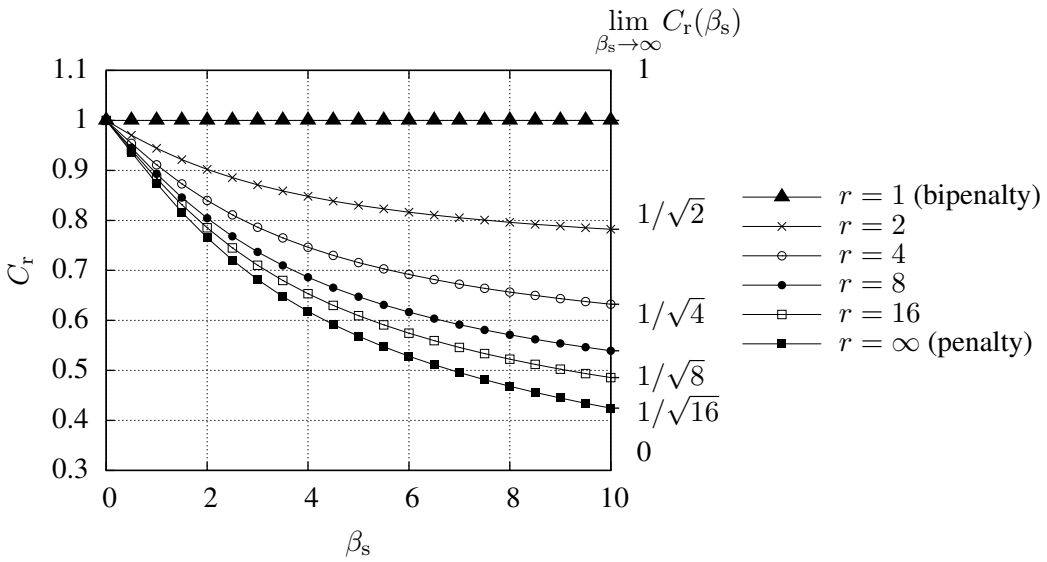

Figure 3: Bipenalized Signorini problem: Dependence of the critical Courant number C_r on the dimensionless stiffness penalty β_s for selected dimensionless penalty ratios r [9].

rapidly decreases with larger value of stiffness parameters. On the other side, the stability limit for a special setting of ratio of stiffness and mass penalty parameters is not affected by the stiffness penalty term, see line for $r = 1$ in Fig. 3. It means that the stability limit of a contact problem using the bipenalty stabilization is the same as stability of a contact-free problem. Further, the stability limit can be estimated before activation of contact constrains during computations.

Stabilized explicit time integration scheme for contact-impact problems is mentioned in depth. In the work of Wu [15], the fully explicit time integration scheme with stabilized technique for contact-impact problems has been published and tested. The mentioned time integration scheme takes the following flowchart with splitting bulk and contact accelerations:

- Given $\mathbf{u}^t$, $\dot{\mathbf{u}}^{t-\Delta t/2}$, $\mathbf{f}^t_{ext}$
- Compute accelerations of predictor phase $\ddot{\mathbf{u}}^t_{pred} = \mathbf{M}^{-1}(\mathbf{f}^t_{ext} - \mathbf{K}\mathbf{u}^t)$
- Mid-point velocities of predictor phase $\dot{\mathbf{u}}^{t+\Delta t/2}_{pred} = \dot{\mathbf{u}}^{t-\Delta t/2} + \Delta t \ddot{\mathbf{u}}^t_{pred}$
- Displacements of predictor phase $\mathbf{u}^{t+\Delta t}_{pred} = \mathbf{u}^t + \Delta t \dot{\mathbf{u}}^{t+\Delta t/2}_{pred}$
- For given $\mathbf{u}^{t+\Delta t}_{pred}$ analyze contact, compute gap vector $\mathbf{g}$ and contact forces $\mathbf{f}_\mathrm{cont} = -\mathbf{K}_\mathrm{p}\mathbf{u}^{t+\Delta t}_{pred} + \mathbf{f}^0_\mathrm{p}$
- Compute accelerations of corrector phase $\ddot{\mathbf{u}}^t_{corr} = (\mathbf{M} + \mathbf{M}_\mathrm{p})^{-1}(\mathbf{f}_\mathrm{cont})$
- Compute total accelerations $\ddot{\mathbf{u}}^t = \ddot{\mathbf{u}}^t_{pred} + \ddot{\mathbf{u}}^t_{corr}$
- Mid-point velocities of corrector phase $\dot{\mathbf{u}}^{t+\Delta t/2} = \dot{\mathbf{u}}^{t+\Delta t/2}_{pred} + \Delta t \ddot{\mathbf{u}}^t_{corr}$
- New displacements of corrector phase $\mathbf{u}^{t+\Delta t} = \mathbf{u}^t + \Delta t \dot{\mathbf{u}}^{t+\Delta t/2}$
- For given $\mathbf{u}^{t+\Delta t}$ analyze contact, compute gap vector $\mathbf{g}$ and contact forces $\mathbf{f}^{t+\Delta t}_\mathrm{cont} = -\mathbf{K}_\mathrm{p}\mathbf{u}^{t+\Delta t} + \mathbf{f}^0_\mathrm{p}$
- $t \to t + \Delta t$

In this two-time step scheme, bulk accelerations in the predictor phase $\ddot{\mathbf{u}}^t_{pred}$ are computed only for internal and external forces without information about contact constrains and they are computed with the standard lumped mass matrix as for a contact-free problem. After updating of velocities and displacements, contact constraints are analyzed and contact forces $\mathbf{f}_\mathrm{cont}$ are computed. For these contact forces, contact accelerations in the corrector phase $\ddot{\mathbf{u}}^t_{corr}$ are computed with the additional penalized mass matrix. After that, the both parts of accelerations are taken together.

In Figs. 5, one can see time histories of contact forces between two elastic bars from Fig. 4 computed by the stabilized explicit scheme. In this cases, the bipenalty method with the optimal ratio of

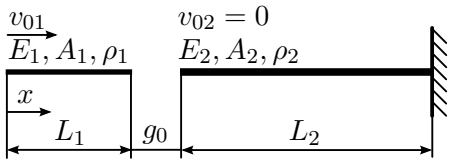

Figure 4: A scheme of an one-dimensional impact of two bars with different lengths.

stiffness and mass penalty parameters were used. The time histories are presented for several values of dimensionless stiffness penalty parameter as follows $\beta_s = \{0.25;\ 0.25e2;\ 0.25e4;\ 0.25e8\}$. One can see that results for $\beta_s = 0.25$ exhibit excellent progress, because this value of β_s corresponds to stiffness of the finite element in contact. On the other hand, the results of the central difference method for higher value of β_s shown significant spurious oscillations of contact forces, where force amplitudes grow up with the value of stiffness penalty parameter β_s. In Fig. 5, the results for the stabilized explicit scheme are presented for higher values of β_s. In principle, for higher β_s, one can see the contact force histories independent of β_s. Further, the stabilized explicit scheme produces robust and stable results for contact forces for a large range of stiffness penalty parameters including extremely higher values.

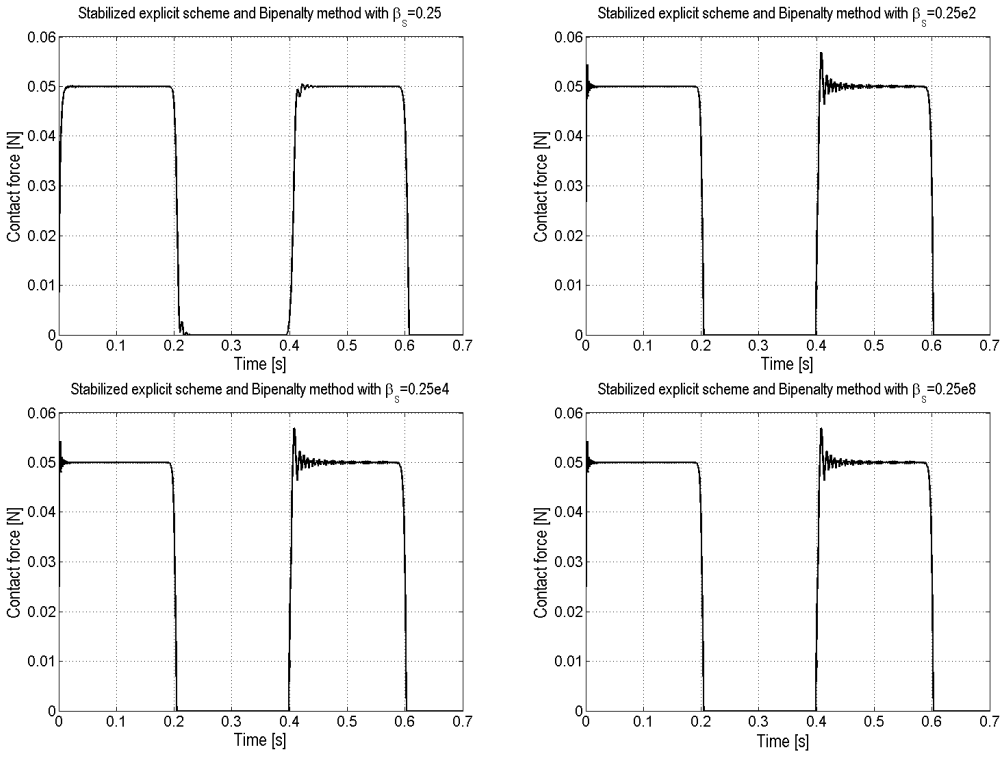

Figure 5: Time history of contact force for impact of two bars with different lengths - the stabilized explicit method with Courant number $C = 0.5$ for $\beta_s = \{0.25;\ 0.25e2;\ 0.25e4;\ 0.25e8\}$ and optimal bipenalty stabilization setting.

3.3 Direct inversion of mass matrix

In the explicit time integration is needed to solve the system (1) in each time step. One can solve the system using the inverse mass matrix $\mathbf{M}^{-1}$ as

$$\mathbf{a} = \mathbf{M}^{-1}\mathbf{F}, \tag{18}$$

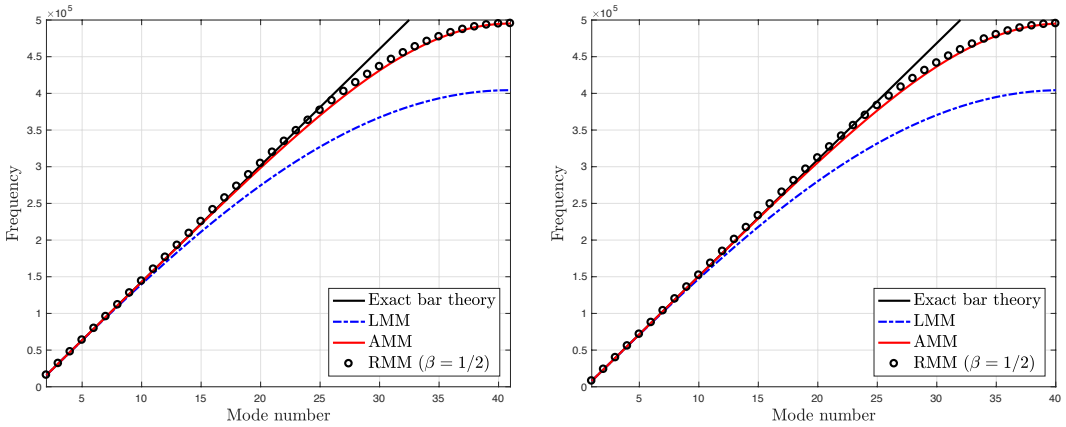

Figure 6: Bar vibration problem. Frequencies for the free-free (left) and fixed-free (right) cases. Comparison of exact frequencies and numerical frequencies obtained with: lumped mass-matrix (LMM), average mass-matrix (AMM) and the proposed inverse mass-matrix (RMM).

but in the case of off-diagonal (e.g. consistent) mass matrix and a large problem the process is not effective. If one solve a linear problem, the inversion of $\mathbf{M}$ is evaluated only at the beginning of computational process.

Approximation of inversion of the mass matrix is called the reciprocal mass matrix and in works of Tkachuk [16] and Gonzalez [10], it has been suggested to evaluated as

$$\mathbf{M} = \mathbf{A}\mathbf{C}^{-1}\mathbf{A}^{\mathrm{T}} \Rightarrow \mathbf{M}^{-1} = \mathbf{A}^{-1}\mathbf{C}\mathbf{A}^{-\mathrm{T}} \tag{19}$$

where $\mathbf{A}$ is the global projection matrix and $\mathbf{C}$ is the global reciprocal mass matrix. Often, the matrix $\mathbf{A}$ is chosen as diagonal and after that the inversion is a trivial issue and only inversion of elemental mass matrices in needed. In the work [10], the element-by-element evaluation of the reciprocal mass matrix (RMM) is presented and tested in free vibration problems. In Fig. 6, the comparison of frequency spectra is depicted. One can see very good agreement of spectrum for the reciprocal mass matrix and the averaged mass matrix (a linear combination of consistent and lumped mass matrix).

4 Conclusions

The three recent and novel methods for improving of explicit time integration in finite element analysis have been presented and tested in one-dimensional problems. In the future, the work will be extended into mutli-dimensional problems and all presented methods will be taken together for modelling of complex geometrical and material dynamic problems with contact constrains with friction.

Acknowledgement

The work of was supported by the Centre of Excellence for Nonlinear Dynamic Behaviour of Advanced Materials in Engineering CZ.02.1.01/0.0/0.0/15_003/0000493 (Excellent Research Teams) in the framework of Operational Programme Research, Development and Education. Further, the work of was supported by the grant projects with No. 17-22615S and No. 17-12925S of the Czech Science Foundation (CSF) within institutional support RVO: 61388998.

References

[1] Hughes TJR. *The Finite Element Method: Linear and Dynamic Finite Element Analysis*. Dover Publications: New York, 2000.

[2] Belytschko T, Hughes TJR. *Computational Methods for Transient Analysis*. North-Holland: Amsterdam, 1983.

[3] Zhong Z. *Finite Element Procedures for Contact-Impact Problems*. Oxford science publications. Oxford, England: Oxford University Press, 1993.

[4] Dokainish MA, Subbaraj K. A survey of direct time-integration methods in computational structural dynamics - I. Explicit methods. *Computers & Structures*, 1989, **32**(6), 1371-1386.

[5] Belytschko T, Liu, WK, Moran B. *Nonlinear finite elements for continua and structures*. Wiley, 2008.

[6] Park KC. Practical aspect of numerical time integration. *Computures & Structures*. 1977, **7**, 343-353.

[7] Fried I. Bounds on the extremal eigenvalues of the finite element stiffness and mass matrices and their spectral condition number. *Journal of Sound and Vibration*, 1972, **22**, 407-418.

[8] Kolman R, Cho SS, Park KC, Gonzalez J. An explicit time scheme with local time stepping for one-dimensional wave and impact problems in layered and functionally graded materials. In: *TCOMPDYN 2017. 6th International conference on computational methods in structural dynamics and earthquake engineering*. Proceedings. Athens: National Technical University of Athens, 2017, (Papadrakakis, M.; Fragiadakis, M.), p. 1297-1303. ISBN 978-618-82844-1-8.

[9] Kopačka J, Tkachuk A, Gabriel D, Kolman R, Bischoff M, Plešek J. On stability and reflection-transmission analysis of the bipenalty method in impact-contact problems: a one-dimensional, homogeneous case study, International *Journal for Numerical Methods in Engineering*, 2018, **113**(10), 1607-1629.

[10] Gonzalez J, Kolman R, Cho SS, Felippa C, Park KC. Inverse Mass Matrix via the Method of Localized Lagrange Multipliers. *International Journal for Numerical Methods in Engineering*, 2018, **113**(2), 277-295.

[11] Park KC, Lim SJ, Huh H. A method for computation of discontinuous wave propagation in heterogeneous solids: basic algorithm description and application to one-dimensional problems. *International Journal for Numerical Methods in Engineering*, 2012, **91**, 622-643.

[12] Cho SS, Park KC, Huh H. A method for multidimensional wave propagation analysis via component-wise partition of longitudinal and shear waves. *International Journal for Numerical Methods in Engineering*. 2013, **95**, 212-237.

[13] Kolman R, Cho SS, Park KC. Efficient implementation of an explicit partitioned shear and longitudinal wave propagation algorithm. *International Journal for numerical Methods in Engineering*. 2016, **107**(7), 543-579.

[14] Kolman R, Plešek K. Červ J, Okrouhlí M, Pařík P. Temporal-spatial dispersion and stability analysis of finite element method in explicit elastodynamics.
International Journal for Numerical Methods in Engineering. 2016, **106**(2), 113-128.

[15] Wu AR. A priori error estimates for explicit finite element for linear elasto-dynamics by Galerkin method and central difference method. *Computer Methods in Applied Mechanics and Engineering*. 2000, **192**(81), 5329-5353.

[16] Tkachuk A, Bischoff M. Direct and sparse construction of consistent inverse mass matrices: general variational formulation and application to selective mass scaling. *International Journal for Numerical Methods in Engineering*. 2015, **101**(6), 1097-0207.